Challenge to Geotechnical Earthquake Engineering Frontier: Consideration of Buildings Overturned by the 2011 Tohoku Earthquake Tsunami

Kohji Tokimatsu[1], Michitaka Ishida[2], and Shusaku Inoue[3]

[1] Tokyo Soil Research Co. Ltd., Tokyo 152-0021, Japan
tokimatsu@tokyosoil.co.jp
[2] Shimizu Corporation, Tokyo 104-8370, Japan
ishida.m@shimz.co.jp
[3] Takenaka Corporation, Inzai City, 270-1395, Japan
inoue.shuusaku@takenaka.co.jp

Abstract. A simplified pseudo-static analysis is proposed to estimate the safety factors with time against instability of a building subjected to tsunami loads, based on the results of a 2D shallow water equation. The proposed analysis is used to examine the key factors affecting the performance of buildings. A 3D analysis is also conducted for one building, the performance of which has not been explained by the simplified analysis. It is shown that: (1) if the tsunami hydrodynamic and buoyant forces are the major driving forces, the proposed analysis is capable of predicting the difference in observed building performance; (2) the safety factors against overturning and sliding become minima near when the peak landward and seaward flow velocities occur, while one against uplift around when the peak inundation depth occurs; (3) the instability of building tends to occur when any of the safety factors first becomes less than one, i.e., mostly at the peak landward flow velocity; (4) the hill immediately backward of a building might have induced a lower peak landward flow velocity at a lower inundation depth and a peak seaward flow velocity at a deeper inundation depth than any other location, having affected the seaward overturning of the building; (5) the major cause of the overturning in orthogonal to the tsunami propagation direction of one building is likely due to the collision of the drifting section of other building originally located on the seaside; and (6) the interdisciplinary collaboration was enormously useful to the progress of this study.

Keywords: Tsunami Load, Overturning of Building, 2011 Tohoku Earthquake.

1 Introduction

The tsunami caused by the 2011 Tohoku Earthquake induced catastrophic damage to various structures along the east Japanese coast. In particular, many buildings even including those supported on pile foundations were overturned and swept away in the

town of Onagawa [7, 12-14], the location of which is shown in Figure 1(a). The overturning direction of those buildings was mainly landward or occasionally seaward, i.e., parallel to the tsunami hydrodynamic force, or even rarely parallel to the shoreline, i.e., orthogonal to the tsunami hydrodynamic force. Sugimura et al. [12] indicated several factors that might have caused the overturning of buildings, such as hydrodynamic and buoyant forces, scour, liquefaction of underlying soil, and debris impact. It seemed important to identify the key factor controlling the problem but difficult to do so without interdisciplinary perspectives including a geotechnical viewpoint. The motivation of this study is therefore to identify the key factors differentiating the occurrence, timing, and direction of overturning based on interdisciplinary collaboration.

A simplified pseudo-static analysis is presented, for this purpose, to estimate the factors of safety with time against overturning, sliding, and uplift of a building, based on the time histories of inundation depth and flow velocity predicted by a two-dimensional shallow water analysis. The proposed analysis is then applied to examine the key factors controlling five buildings, the field performances of which are known. A three-dimensional shallow water analysis is also conducted for one building, the overturning reason of which has not been explained by the simplified pseudo-static analysis.

2 Field Performance of Target Buildings

Figure 1(b) shows a map of Onagawa town before the tsunami [2] with the area inundated by the 2011 Tohoku Earthquake tsunami [4] as well as the locations of five Buildings A to E examined in this study.

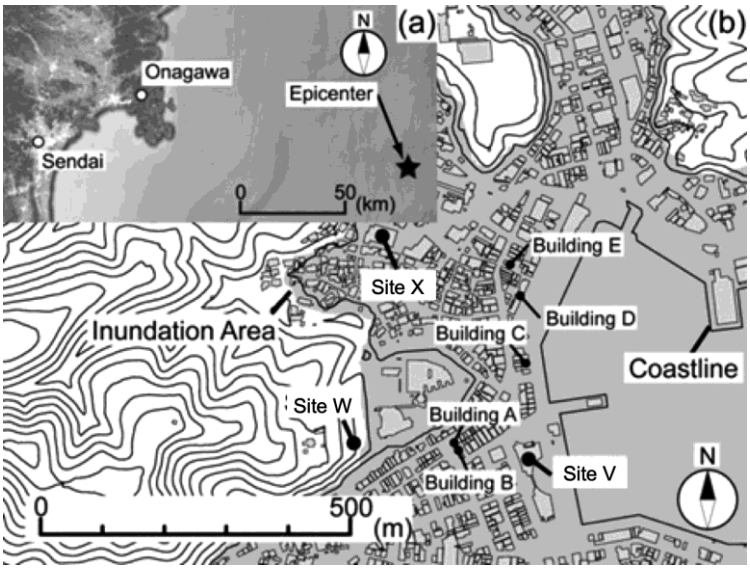

Fig. 1. Location of (a) Onagawa and (b) investigated buildings with inundation area

Figure 2 is an aerial photograph of the hardest hit area in Onagawa taken after the tsunami [2], which shows the locations of the buildings before and the after the event. Building A and D overturned landward, Building C overturned seaward, and Building E overturned almost in parallel to the coastline, while Building B remained at its original position. Digital recording open for public including the video taken from Site V [9] and photos taken from various places including Sites W and X [10, 15] has shown that Buildings A and D overturned during the first tsunami runup and Buildings C and E by the end of the first tsunami backwash.

Figure 3 shows Building A, a four-story RC building with pile foundation that over-

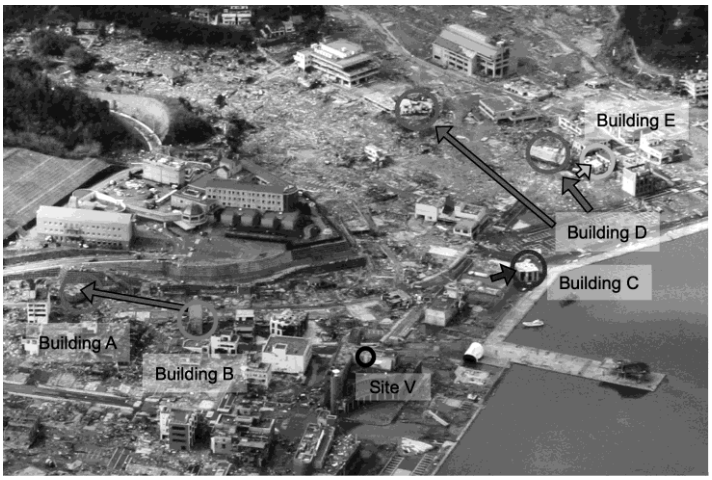

Fig. 2. Location and overturning direction of buildings investigated (Photo [2])

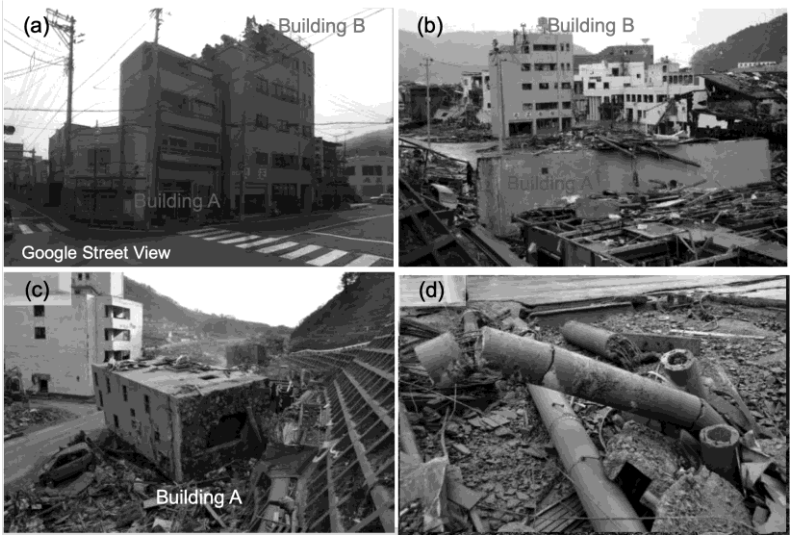

Fig.3. Photos of Buildings A and B taken before and after tsunami (Photo (a) [3])

turned landward during the first tsunami runup and displaced landward by 70 m from its original position. This building had been supported on 32 RC piles 4m long and 300mm in diameter (Figures 3(a) and 3(b)). All piles except one pile hanging down from the building (Figure 3(c)) were broken and cut at or near the pile head. Some of those piles were pulled up to 3m at its original position (Figure 3(d)), and the exposed steel reinforcement had cut remaining thinning ends. The difference in failure mode among piles suggests that the overturning of this building progressively occurred in a certain period of time.

Figures 3(a) and 3(b) also show Building B, a five-story RC building founded on piles that survived at its original position. The ground subsidence around the building indicated the occurrence of soil liquefaction, the influence of which was considered to be insignificant, considering that the pullout resistance of piles of Building A was almost mobilized.

Figure 4 shows Building C, a four-story RC building with spread foundation, which is the only one in the town having overturned seaward. The fourth floor of the building detached and was missing.

Figure 5 shows Building D, a three-story RC building with spread foundation that toppled, split into two or three sections, and drifted landward during the first tsunami runup. While the left section seen in Figure 5(a) was found about 175 m landward from its original position (Figure 2), the right section only about 75 m landward near Building E (Figures 2 and 5(b)).

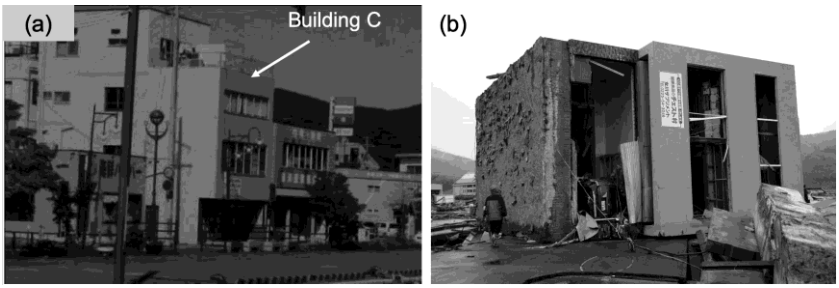

Fig.4. Photos of Building C taken before and after tsunami

Fig.5. Photos of Building D taken before and after tsunami (Photo (a) [15])

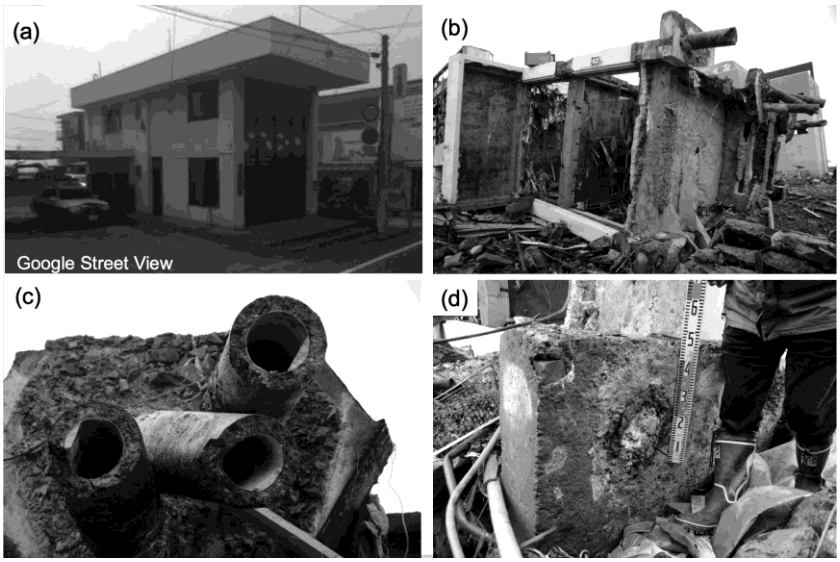

Fig. 6. Photos of Building E taken before and after the tsunami (Photo (a) [3])

Figure 6 shows Building E, a two-story RC building that toppled parallel to the shoreline, i.e., orthogonal to the tsunami propagation direction. It was supported on 14 PC piles 20m long and 300mm in diameter [11]. Either the pile head (Figure 6(d)) or 0.9m to 1.5m below the pile head (Figures 6(b) and 6(c)) failed in a tensile, bending, or compressive mode. This failure mode is completely different from that observed in Building A, suggesting that the failure of the piles and subsequent overturning of the building might have occurred instantly by a much larger driving force.

Table 1 summarizes the general information of the buildings, in which W is the estimated weight, H is the height, B is the width in parallel to the coastline, L is the length perpendicular to the coastline, and D_f is the depth of foundation embedment. Further information about the buildings are found elsewhere [7, 14].

Table 1. General information of buildings investigated

Building ID	W (MN)	H (m)	B (m)	L (m)	D_f (m)	Foundation Type	Pile Diam. (m)	Pile Length (m)
A	2.5	12.4	7.3	5.5	0.9	Pile	0.3	4
B	6.2	17.1	13.0	6.5	0.9	Pile	0.3[1)]	4[1)]
C	3.8	9.5	6.7	10.4	0.6	Spread	-	-
D	32.4	9.0	59.4	11.8	0.9	Spread	-	-
E	1.9	6.3	5.0	11.0	0.6	Pile	0.3	20

1) Assumed

3 Method to Estimate Occurrence of Overturning of Building

3.1 Simplified Method for Estimating Tsunami-induced Overturning of Building

Figure 7(a)-(c) show simplified force diagrams for overturning, sliding, and uplift of a building subjected to tsunami-induced hydrodynamic and buoyant forces. In order to maintain the stability of the building against overturning shown in Figure 7(a), the driving moment induced by both the tsunami hydrodynamic and buoyant forces with respect to the rotational center should be always less than the resisting moment induced either the pullout resistance and the self-weight of a building with piles or the self-weight of a building with spread foundation. The pullout resistance of a building with piles is likely either the skin friction of the piles or the tensile strength of their rebars, whichever is smaller. For the sliding shown in Figure 7(b), the tsunami hydrodynamic force should be always less than either the shear strength of the rebar of piles and the passive earth pressure acting the embedded foundation for a building with piles or the base friction and passive earth pressure for a building with spread foundation. For the uplift shown in Figure 7(c), the tsunami buoyant force should be always less that either the pullout resistance of a building with piles or the self-weight of a building with spread foundation.

The hydrodynamic force F_D acting on a building in the travel direction of tsunami at time t may be calculated by the following formula [1];

$$F_D(t) = \frac{1}{2}\rho C_D u(t)^2 h(t) B \tag{1}$$

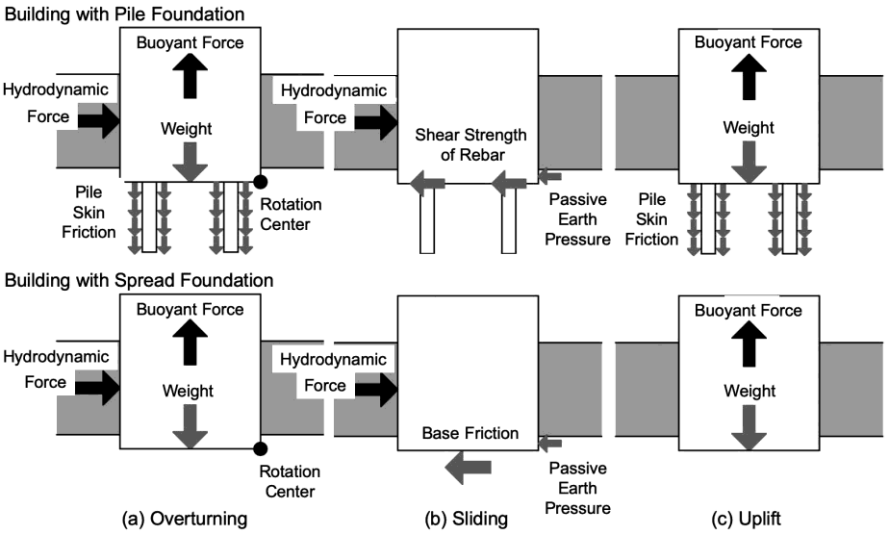

Fig. 7. Simplified free body diagrams for (a) overturning, (b) sliding, and (c) uplift mechanisms of buildings with pile or spread foundation

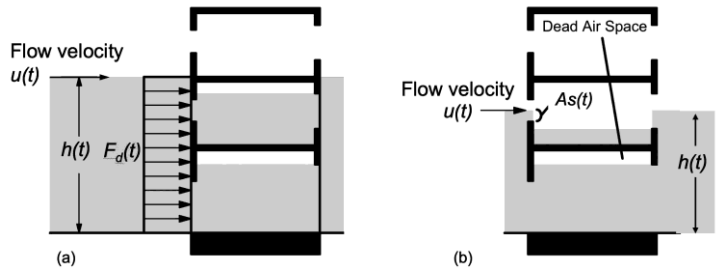

Fig. 8. Comparison of computed (a) inundation depth and (b) flow velocity with observed ones

where t is the time, ρ is the fluid density including sediment (1.2t/m^3), C_D is the drag coefficient (2.0), u and h are the flow velocity and inundation depth computed by the 2D simulation for a given depth such as those shown in Figure 8(a), and B is the build ing width.

The buoyant force F_B acting on a building at time t is calculated by the following formula;

$$F_B(t) = \rho g\{V(t) - V_W(t)\} \tag{2}$$

where g is gravitational acceleration (9.8m/s^2), V is the volume of the building below the inundation depth, and V_W is the volume of water having entered the building.

The flow rate of the water entering the building, $\Delta V_W(t)$, during the tsunami runup was estimated by multiplying the area of the building openings between the interior and exterior inundation depths, $A_s(t)$, by the current flow velocity, $u(t)$, as shown in Figure 8(b). The height to be filled by water in each floor was limited by either the inundation depth or the highest height of the opening of the floor that creates dead air space above, whichever is lower. $V_W(t)$ during the backwash was assumed to be equal to the volume inside the building below the inundation depth, $h(t)$, regardless of the current flow velocity, $u(t)$, and the presence of dead air space during runup. The value of V_W was also constrained by assuming that the dimension of pillar cross-section was 500mm × 500mm and the wall thickness was 200mm.

The method how to evaluate other information including the base horizontal resistances of the building, the passive earth pressure acting on the embedded part of the building, and the pile pullout resistance is found elsewhere [14].

3.2 Estimation of Tsunami Hydrodynamic and Buoyant Forces by 2D Analysis

A 2D analysis of the tsunami runup was conducted with a shallow water theory [6] to estimate the variation with time of the inundation depth and flow velocity around the target buildings, which are needed in Equations (1) and (2). Figure 9 shows two areas used for 2D analysis, which has a dimension of either 1530 m and 570 m or 2960m and 3660m with a uniform mesh of 10m by 10m. Area A shown in Figure 9(a) was used for

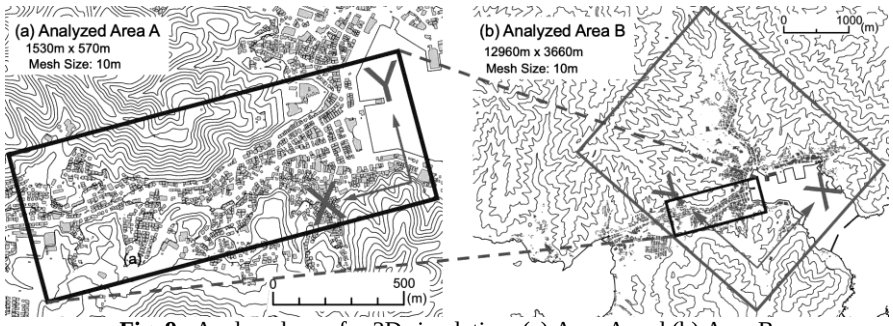

Fig. 9. Analyzed area for 2D simulation: (a) Area A and (b) Area B

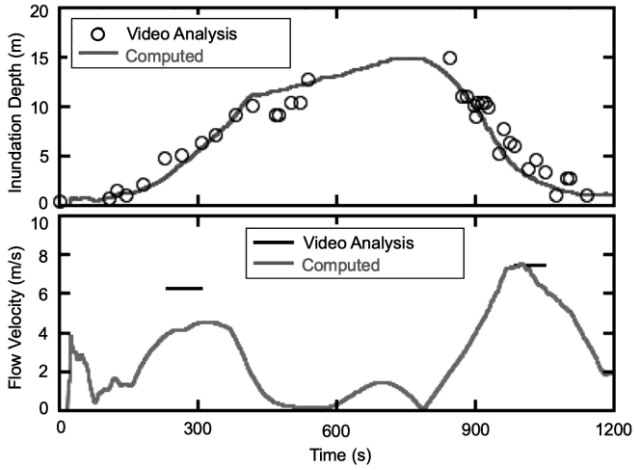

Fig. 10. Comparison of computed and observed (a) inundation depth and (b) flow velocity at Site V

Buildings A-C, while Area B for Buildings D and E, so that Site V, the video observation point, is included in both areas. The terrain model using the 2D analysis was assigned according to the digital elevation model (DEM) provided by the GSI [2] and General Ground Plan of Onagawa Port, Miyagi, available from Japan Center for Asian Historical Records [8].

The open circles in Figure 10(a) are the inundation depth evaluated from the video recording taken at Site V in Figure 1(b) during the first tsunami runup and backwash (Koshimura et al., [9]). The two solid black lines in Figure 10(b) are the peak flow velocities at around 300 s during the first tsunami runup and at around 1000 s during the first tsunami backwash, estimated from the same video recording [9]. The smoothed time history of the estimated inundation depth plus the elevation of Site V was used as the time history of the sea water level prescribed at the seaside boundary of each analyzed area for the tsunami analysis.

Figures 10(a) and (b) show the computed time history of inundation depth and flow velocity at Site V from the analysis for Area A. The computed time history of

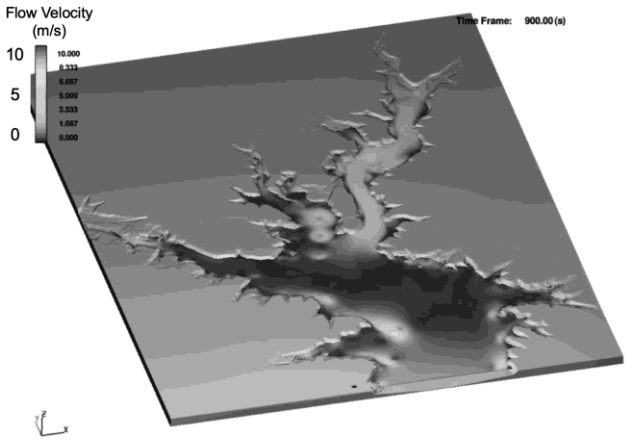

Fig. 11. Computed inundation depth and flow velocity within analyzed area B at 900 s

inundation depth shown in Figure 10(a) corresponds reasonably well to the observed one. The computed flow velocities shown in Figure 9(b) also show fairly good agreements with the observed ones at the two instances. A good agreement between the observed and computed values were also found from the analysis for Area B.

Figure 11 shows a snap of the distribution of inundation depth and flow velocity within Area A at 900 s when the inundation depth took a peak during the first tsunami runup. The computed inundation area is consistent with that observed in the field (Figure 1(b)). Thus, the computed time history of inundation depth and flow velocity at each building location is used to estimate the driving moment and forces with time to be imposed on each building.

4 Comparison of Field Performance with Estimated Result

4.1 Estimation of Field Performance based on 2D Analysis

Figures 12 shows the estime histories of the driving forces/moment and resisting forces/moment for overturning, sliding, uplift for Building A. Note that the ordinate

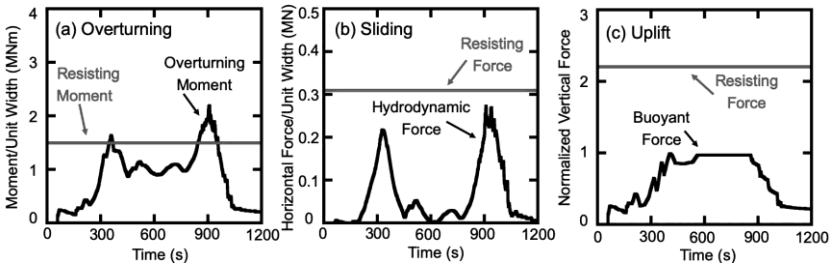

Fig. 12. Comparison between estimated driving and resisting loads to Building A with respect to (a) overturning, (b) sliding, and (c) uplift mechanisms

values in the overturning and sliding diagrams are normalized to the building width, while in the uplift diagram to each building weight.

Figures 13-17 show the time histories of safety factors against overturning, sliding, uplift for the five buildings, in which each safety factor is defined as the ratio between the corresponding driving and resisting loads for each building such as shown in Figure 12.

The safety factors against overturning of Buildings A and D shown in Figures 13 and 16 become less than one at around 300-500 s, suggesting that those buildings could have overturned landward about when the landward flow velocity took a peak as shown in Figure 10(b); which is consistent with the actual field performance of those buildings.

The safety factors against overturning and sliding of Building C shown in Figure 15 become less than one only after 900s about when the seaward flow velocity took a

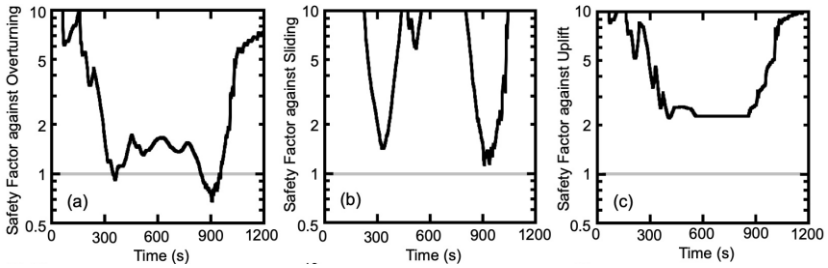

Fig. 13. Computed safety factors against (a) overturning, (b) sliding, and (c) uplift for Building A

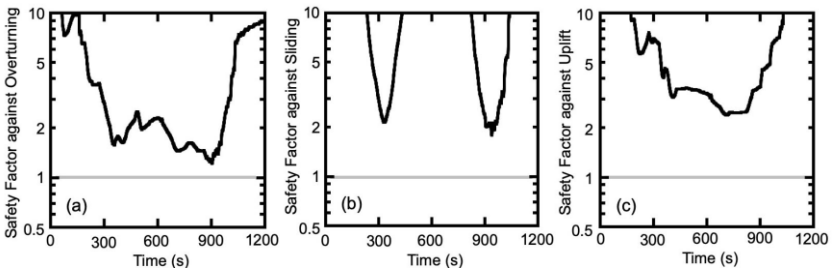

Fig. 14. Computed safety factors against (a) overturning, (b) sliding, and (c) uplift for Building B

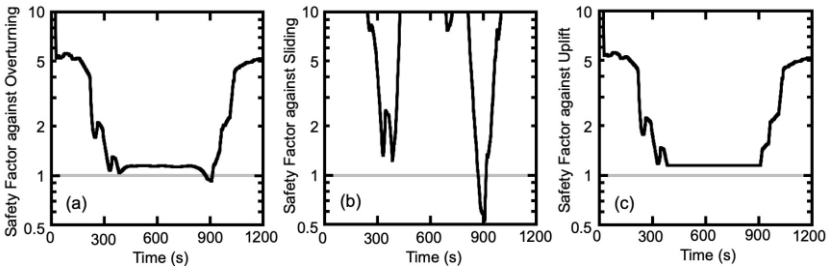

Fig. 15. Computed safety factors against (a) overturning, (b) sliding, and (c) uplift for Building C

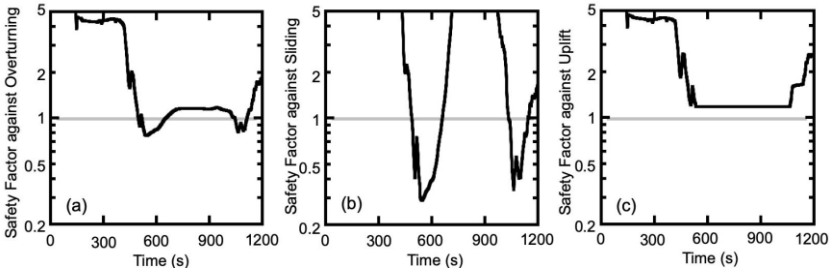

Fig. 16. Computed safety factors against (a) overturning, (b) sliding, and (c) uplift for Building D

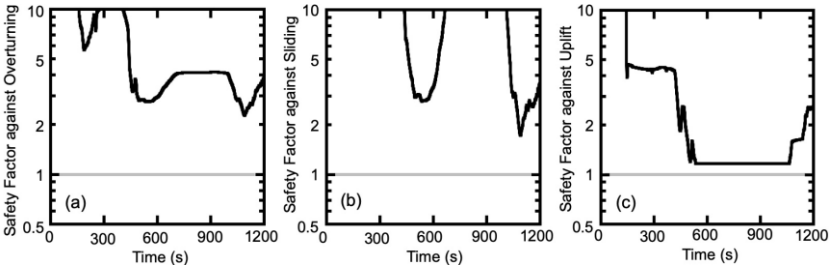

Fig. 17. Computed safety factors against (a) overturning, (b) sliding, and (c) uplift for Building E

peak as shown in Figure 9(b), which is consistent with the seaward overturning of this building.

Any of the safety factors of Building B shown in Figures 14, in contrast, is always greater than one, confirming that this building could have survived tsunami impacts. Similarly, any of the safety factors of Building E in Figures 17 is always less than one, suggesting its good field performance but contradicting its actual field overturning behavior. Moreover, since the overturning direction of this building was orthogonal to the direction of tsunami propagation, the actual driving moment and forces imposed in that direction would be far smaller than the computed ones, suggesting effects other than the tsunami direct forces.

The above discussion suggests that the proposed analysis is capable of predicting the difference in field performance of buildings on the condition that the tsunami-induced hydrodynamic and buoyant forces are the only major driving forces. Under this condition, the safety factors against overturning and sliding by the end of the first backwash, tends to take minima twice when the peak landward and seaward flow velocities occur. The overturning of building, therefore, most likely occur near when the peak landward flow velocity occurs unless the safety factor against overturning is greater than one as is the case for Building C.

In order to explore the reason for the seaward overturning of Building C, Figure 18 compares the computed time histories of inundation depth and flow velocity at Buildings A and C. The peak flow velocities at Building C are significantly smaller and occur at a lower inundation depth during runup and at a deeper inundation depth during

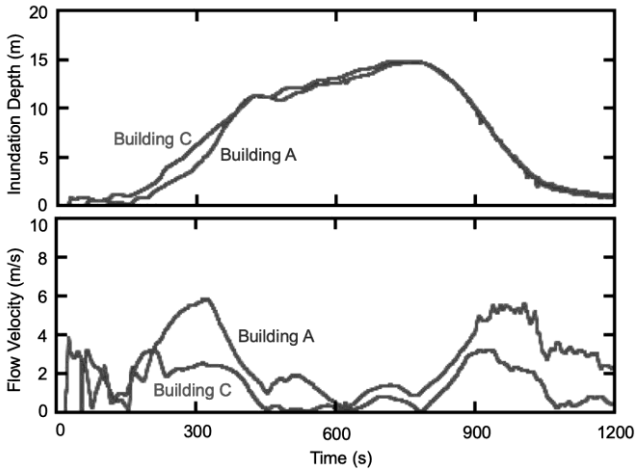

Fig. 18. Computed time histories of (a) inundation depth and (b) flow velocity at Buildings A and C

backwash than those at Building A, probably having led to the seaward overturning of this building. Such variation of flow velocity with time at Building C might have been caused by the presence of a hill immediately located landward of Building C.

4.2 Estimation of Field Performance based on 3D Analysis

The inconsistency between the computed result and the field performance of Building D shown in the previous section motivated us further to examine possible effects other than tsunami induced forces, i.e., the collision impact of drifting Building D on the overturning behavior of Building E.

A 3D analysis was therefore conducted with Volume of Fluid (VOF) method [5] for the restricted area encircled with lines shown in Figures 19(a) and 19(b), which

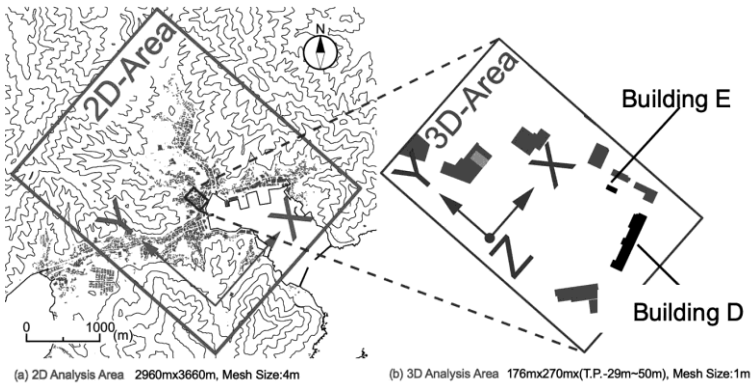

Fig. 19. Analyzed area for 3D simulation: (a) 2D area and (b) 3D area

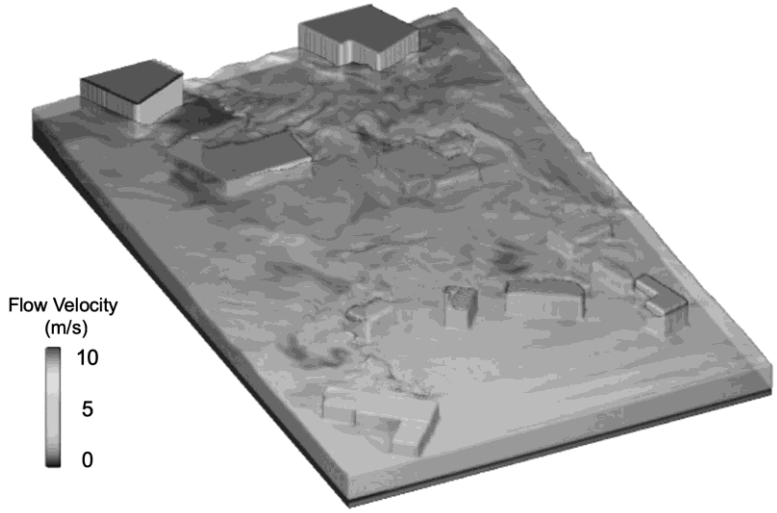

Fig. 20. Variation of computed inundation depth and flow velocity with drifting Building D at t=520 s

has a dimension of 176m and 270m and T.P. 129m to +50m with a uniform mesh of 1m by 1m. The terrain model using the 3D simulation was one used for the 2D analysis described in Section 3.2 plus all surviving and the target buildings (i.e., Buildings D and E). Building D was divided along its longitudinal direction into three sections that can move separately. The coefficient of friction between each section and the ground was assumed to be 0.4. The density of each section was also assumed to be 1.09 t/m^3, which corresponds to the condition where the volume of water in the building is a half of the inside volume of the building. The input boundary conditions prescribed to the seaside of the 3D area shown in Figure 19(b) were the inundation depth and flow velocity computed by the 2D analysis, but using a more precise mesh of 4m by 4m plus all surviving and target two buildings as shown in Figure 19(a). The analysis was conducted only for the tsunami runup phase (until 970s).

Figure 20 shows the variation of computed inundation depth and flow velocity within the area as well as the floating behavior of Building D at times of 520 s. The building started to drift at about 480 s, and the right section of the building hit the southwest side of Building E at about 520 s and remained nearby thereafter. This is consistent with the actual field observation such as shown in Figure 2, suggesting that the overturning of Building E in parallel to the coastline might have occurred due to the collision of the right section of Building D.

Figures 21(a) and 21(b) show the computed time histories of hydrodynamic force acting on the shorter and longer directions (orthogonal and parallel to the tsunami propagation directions) respectively of Building E computed by the 3D simulation. Note that the collision impact force of the right section of Building D to Building

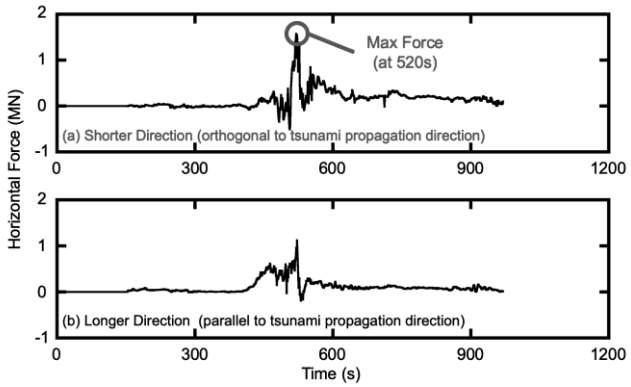

Fig. 21. Computed hydrodynamic forces acting on Building E from 3D analysis: (a) shorter direction and (b) longer direction

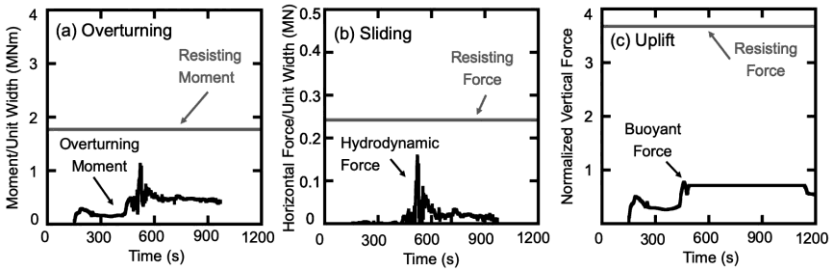

Fig.22. Comparison between estimated driving and resisting loads to Building A with respect to (a) overturning, (b) sliding, and (c) uplift mechanisms

E was not computed directly from the 3D analysis and thus is not included in the computed force. Figures 21(a) and 21(b) suggest that the horizontal force at the time of the collision is larger in the shorter direction than in the longer direction.

The proposed pseudo-static analysis was again performed for Building E along its shorter direction using the hydrodynamic force shown in Figure 21(a). Figure 22 shows the estimated loads and resistances for overturning, sliding, and uplift of the building. The figure suggests that Building E would have overturned if the collision impact force not determined from the 3D analysis is about 2MN.

Taking into account that the weight and velocity as well as the final location of the right section of Building D, its potential collision force to the shorter direction of Building E would be estimated to be greater than 16MN. This is much greater than the critical one (2MN), suggesting that the collision of the right section of Building D is the major factor having induced the overturning of Building E.

Figure 23 shows a photo of the roof of overturned Building E. The serious damage observed on its upper side, previously faced southwest, appears to demonstrate that it was caused by the collision of the right section of Building D having drifted from southwest.

Fig. 23. Serious damage observed on the roof of Building E overturned probably due to collision of Building D [3]

5 Conclusions

In order to clarify the major factors causing the difference in tsunami-induced damage among the five buildings in Onagawa, a simplified pseudo-static analysis was proposed to estimate the factors of safety in the time domain against overturning, uplift, and sliding of a building for which the hydrodynamic and buoyant forces are estimated from the 2D shallow water equations. A three-dimensional shallow water analysis was also conducted for one building, the performance of which had not been explained by the simplified analysis. It was shown that: (1) if the tsunami-induced hydrodynamic and buoyant forces are the major driving forces, the proposed analysis is capable of predicting the difference in observed building performance; (2) the safety factors against overturning and sliding become minima when the peak landward and seaward flow velocities occur, while one against uplift when the peak inundation depth occurs; (3) the overturning of building tends to occur when any of the safety factors first becomes less than one, i.e., mostly at the peak landward flow velocity; (4) the seaward overturning of one building is likely due to the topographical conditions created by the hill immediately backward, which could have made the inundation depth lower at the peak landward flow velocity and deeper at the peak seaward flow velocity than any other location, having caused the safety factor less than one for the first time during backwash; (5) the major cause of the overturning in orthogonal to the tsunami propagation direction of one building is likely due to the collision of the drifting section of other building originally located on the seaside; and (6) the interdisciplinary collaboration was enormously useful to the progress of this study.

Acknowledgements

The most part of this study was made while the first and second authors were a professor and a graduate student of Tokyo Institute of Technology. The various support provided by the university and colleagues is appreciated.

References

1. Federal Emergency Management Agency: Guideline for Design of Structures for Vertical Evacuation from Tsunamis. FEMA P646 (2008).
2. Geospatial Information Authority of Japan (GSI), http://mapps.gsi.go.jp, last accessed 13 January, 2022.
3. Google, Memories for the Future, at http://www.miraikioku.com/, last accessed 13 January, 2022.
4. Haraguchi, T. and Iwamatsu, A.: Detailed Maps of the Impacts of the 2011 Japan Tsunami Vol.1: Aomori, Iwate and Miyagi prefectures, Kokon-Shoin Publishers, 167pp, (2011).
5. Hirt, C.W. and Nicholas, B.D.: Volume of Fluid (VOF) Method for the Dynamics of Free Boundaries. Journal of Computational Physics, 39, pp.201-225 (1981).
6. Hirt, C.W. and Richardson, J.E.: The modeling of shallow flows, Flow Science, Inc., Technical Notes, FSI-99-TN48R (1999).
7. Ishida, M., Tokimatsu, K., and Inoue, S.: Factors Affecting Overturning of Building Induced by Tsunami Run-up in the 2011 Great Tohoku Earthquake, Proc. 16th World Conf. on Earthquake Engineering, Santiago, Chile, Jan. 9-13, Paper No. 3956, 11pp. (2017).
8. Japan Center for Asian Historian Records (JACAR). Attachment, Onagawa Port, Miyagi, general ground plan, Ref.A11112289000, Relevant Documents regarding Cabinet Tohoku Bureau, File of petition documents (two), 1935 (National Archives of Japan), http://www.digital.archives.go.jp/, last accessed 13 January, 2022.
9. Koshimura, S. and Hayashi, S.: Tsunami flow measurement using the video recorded during the 2011 Tohoku tsunami attack, International Geoscience and Remote Sensing Symposium, IEEE international, pp.6693-6696 (2012).
10. Miyagi Prefecture, Great East Japan Earthquake Archive Miyagi - Onagawa Town, available at http://kioku.library.pref.miyagi.jp/onagawa/, last accessed 13 January, 2022.
11. National Institute for Land and Infrastructure Management, Ministry of Land, Infrastructure and Transport, Japan: Damage investigation report of the 2011 Tohoku-Pacific Ocean Earthquake, TECHNICAL NOTE of NILIM, No.674, 565pp. (in Japanese) (2012).
12. Sugimura, Y. and Mitsuji, K.: The survey of buildings overturned and carried out by tsunami, Foundation Engineering and Equipment, Vol. 40, No.12, pp.71-75 (in Japanese) (2012).
13. Tokimatsu, K., Tamura, S., Suzuki, H. and Katsumata, K.: Buildings damage associated with geotechnical problems in the 2011 Tohoku Pacific Earthquake, Soil and Foundation, Vol. 52, No.5, pp.956-974 (2012).
14. Tokimatsu, K., Ishida, M., and Inoue, S. (2016) : Tsunami-Induced Overturning of Buildings in Onagawa during the 2011 Tohoku Earthquake, Earthquake Spectra, Vol. 32, No. 4, pp. 1989-2007.
15. Yahoo, East Japan Earthquake Picture Project, http://archive.shinsai.yahoo.co.jp/, last accessed 13 January, 2022.